Diagnostics of Plasma Dynamics and Magnetism Inside the Sun by Helioseismology

Alexander G. Kosovichev
W.W. Hansen Experimental Physics Laboratory, Stanford University, Stanford, CA 94305, USA

(Received: 8 September 2008 / Accepted: 3 December 2008)

Helioseismology observations from space missions SOHO and Hinode have provided tremendous amount of new information about thermodynamic properties and dynamics of plasma in the solar interior. The helioseismic diagnostics are based on measuring oscillation frequencies and travel times of acoustic waves excited by turbulent convection in subsurface layers. These diagnostics give us new insights into basic physical processes inside the Sun, formation of magnetic structures in the solar plasma and mechanisms of solar and stellar activity. Recent helioseismology results reveal the deep structure of sunspots and associated plasma flows, and also complicated dynamics of emerging magnetic flux tubes and formation of active regions. In particular, the formation and stability of strong concentrations of magnetic field in sunspots is probably associated with converging flow patterns below the surface and the filamentary structure of magnetic fields in the turbulent solar plasma. Similar self-organization MHD processes are likely to happen in other astrophysical plasmas.

Keywords: solar plasma, magnetic fields, dynamo, solar MHD, helioseismology, SOHO, Hinode

1. Introduction

Turbulent magnetized plasma of the solar interior provides an interesting example of dynamo-generated magnetic fields and remarkable self-organization. Despite strong turbulent convective flows that tend to spread magnetic fields, the solar plasma shows a tendency of formation of magnetic sunspots, compact long-living structures of intense magnetic field. Groups of sunspots form active regions that are the primary source of impulsive magnetic energy release events producing high-energy flare particles, X-ray and γ-ray emissions, and mass ejection, presumably due to magnetic reconnection. The mechanism of sunspot formation is a long-standing puzzle. Solving it is important for understanding mechanisms of magnetic self-organization in other astrophysical plasmas. From measurements of surface magnetic fields, which revealed the filamentary structure of sunspots [1], and from theoretical arguments [2] it has been suggested that sunspots represent clusters of magnetic flux tubes bound together by subsurface converging plasma flows. Initial helioseismology observations have provided evidence for such flows around stable sunspots [3], confirming Parker's cluster model (Fig. 1). However, attempts to reproduce the sunspot structure in realistic MHD numerical simulations have not been successful. In the simulations, large-scale magnetic structures are quickly dispersed by convective flows. The converging flows similar to the observations are reproduced in simulations of cylindrical magnetic structures [4], but in the full 3D simulations [5] the converging flows seem to be rather weak and do not prevent spreading of magnetic structures by the turbulent convection. Thus, there seem to be some additional factors that are essential for the existence of sunspots. In this paper, we discuss new results of helioseismic investigations of the process of emergence of magnetic flux and formation of sunspots. These results lead to the idea that the stability of sunspots can be provided by a subsurface dynamo source that keeps pumping magnetic flux in compact local areas.

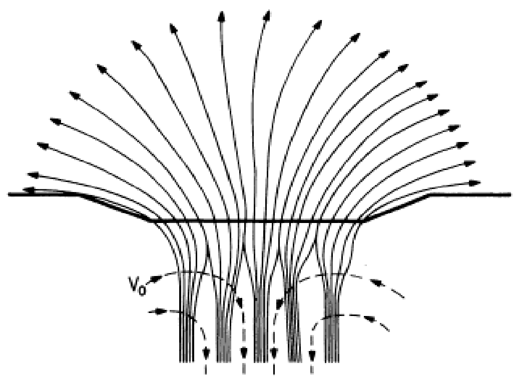

Fig. 1 Illustration of the cluster model of sunspots [2]

2. Method

We use a diagnostic method of acoustic tomography or time-distance helioseismology (e.g. [6, 7, 8, 9]) to investigate the structure and dynamics below the visible surface of the Sun. This method is based on measurements of travel times of acoustic waves traveling through the solar interior between different points on the surface. The travel times depend on the wave speed along the wave paths, and, thus, can be used to infer the distributions of the wave-speed and flow

author's e-mail: sasha@sun.stanford.edu

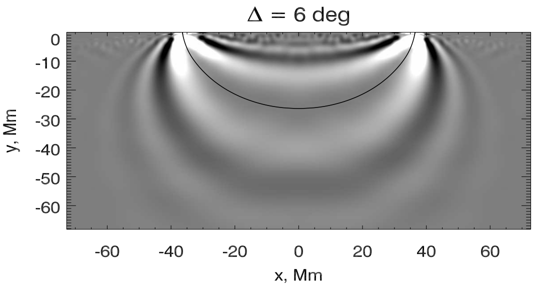

Fig. 2 Travel time sensitivity functions in the Born approximation. The solid curves show the corresponding ray paths.[11]

velocities.

Solar acoustic waves are excited stochastically by turbulent convection. Therefore, the wave travel time and other wave propagation properties are determined from the cross-covariance function, $\Psi(\tau, \Delta)$, of the oscillation signal, $f(t, \boldsymbol{r})$, measured at different locations on the solar surface:

$$\Psi(\tau, \Delta) = \frac{1}{T} \int_0^T f(t, \boldsymbol{r}_1) f^*(t + \tau, \boldsymbol{r}_2) \mathrm{d}t, \quad (1)$$

where Δ is the angular distance between the points with coordinates $\boldsymbol{r}_1$ and $\boldsymbol{r}_2$, τ is the delay time, and T is the total time of the observations. Function Ψ must be averaged over some areas on the solar surface to achieve a good signal-to-noise ratio, sufficient for measuring travel times τ. The oscillation signal, $f(t, \boldsymbol{r})$, is usually the Doppler velocity of the surface plasma or intensity fluctuations.

The travel-time variations can be related to perturbations of the wave speed, $\delta c/c$, and the flow velocity, $\boldsymbol{U}$, via a linear integral equation:

$$\delta\tau = \int_V K_c \frac{\delta c}{c} \mathrm{d}V + \int_V (\boldsymbol{K}_u \cdot \boldsymbol{U}) \mathrm{d}V, \quad (2)$$

where $K_c(\boldsymbol{r})$ and $\boldsymbol{K}_u(\boldsymbol{r})$ are sensitivity functions for $\delta c/c$ and $\boldsymbol{U}$; the integration is carried over the interior volume, V.

The sensitivity kernels are derived by using some approximations, e.g. the ray theory or the first Born approximation. In the Born approximation, the sensitivity kernels can be expressed in terms of the unperturbed eigenfunctions of solar oscillation modes [10, 11]. Examples of the Born sensitivity kernels for wave-speed perturbations are shown in Fig. 2.

In the ray-theoretical approximation, which is still often used for helioseismic inferences, the first-order perturbations to the phase travel time is given by [9]:

$$\delta\tau = -\int_\Gamma \left[\frac{(\boldsymbol{n} \cdot \boldsymbol{U})}{c^2} + \frac{\delta c}{c} S + \left(\frac{\delta\omega_c}{\omega_c} \right) \frac{\omega_c^2}{\omega^2 c^2 S} \right] \mathrm{d}s \quad (3)$$

where $\delta c/c = \delta c_s/c_s + \frac{1}{2}\left[c_A^2/c^2 - (\boldsymbol{k} \cdot \boldsymbol{c_A})^2/k^2c^2\right]$ is the variation of the fast magnetoacoustic speed, $\boldsymbol{n}$ is a unit vector tangent to the ray, $S = k/\omega$ is the phase slowness, $\boldsymbol{k}$ is the wave vector and k its magnitude, ω_c is the acoustic cut-off frequency, $\boldsymbol{c_A} = \boldsymbol{B}/\sqrt{4\pi\rho}$ is the vector Alfvén velocity, $\boldsymbol{B}$ is the magnetic field strength, c_s is the adiabatic sound speed, and ρ is the plasma density. The integration is performed along the unperturbed ray path Γ according to Fermat's principle [12]. The effects of flows and structural perturbations are separated by taking the difference and the mean of the reciprocal travel times. Magnetic field causes anisotropy of the mean travel times, which allows us to separate, in principle, the magnetic effects from the variations of the wave speed (or temperature).

3. Magnetic flux emergence and formation of sunspots

Using the method of time-distance helioseismology, we have obtained wave-speed and flow velocity maps for 8 days, 25–31 October, 2003, using data from the MDI instrument on the Solar and Heliospheric Observatory (SOHO)[13]. The maps are obtained using 8-hour time series with a 2-hour shift. Total 96 wave-speed and flow maps were obtained [14]. Figure 3 shows a sample of the wave-speed images. The results show that the first wave-speed signal below the surface and the first magnetic field on the surface appeared approximately at the same time. During the next 8 hours, the perturbation rapidly grows, and is most visible in the subsurface layers, about 10 Mm deep. In the deeper interior, we do not detect a clear signal above the noise level at this time. This may be because the relative perturbation in these layers is too weak, and also may indicate that the formation of magnetic flux concentrations starts in the subsurface layers. During the next 8 hours the signal extends into the deeper layers and continues to grow. A typical two-layer structure with lower wave speed in the top 4–5 Mm (Fig. 3d), and higher wave speed in the deeper layers is formed [15, 16, 17]. During the following 5 days of the MDI observations, the wave-speed perturbation below the active region becomes larger and stronger, and in the East-West direction it forms a loop-like structure (Fig. 3c). This structure can be traced to the depth of about 30 Mm, and then it is lost in noise.

The helioseismology measurements of subsurface flows are obtained from the reciprocal travel times, and, generally, are less affected by various kind of uncertainties. They may provide better indicators of the development of active region structures inside the Sun. Figure 4 shows three flow maps at the depth of about 2 Mm for various stages of evolution of the active region, NOAA 10488, before the emergence, during the initial emergence, and during the developed state. The

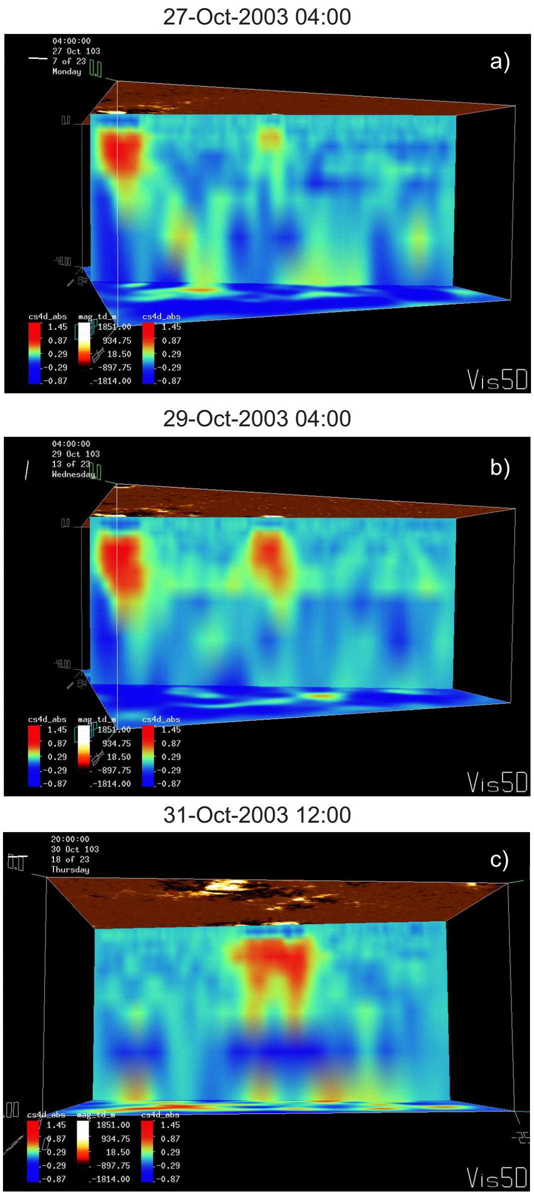

Fig. 3 Subsurface magnetosonic wave-speed structures of the large complex of activity of October–November 2003, consisting of active regions NOAA 10486 (in the left-hand part of the images), and 10488 (emerging active region in the middle). Red color shows positive wave-speed variations relative to the quiet Sun; the blue color shows the negative variations, which are concentrated near the surface. The upper semi-transparent panels show the corresponding MDI magnetograms; the lower panel is a horizontal cut 48 Mm deep. The horizontal size is about 540 Mm. The vertical cut goes through both active regions, approximately in the North–South direction, crossing the equator), except the image in the bottom panel, (c), where it goes only through AR 10488 in the East–West direction.

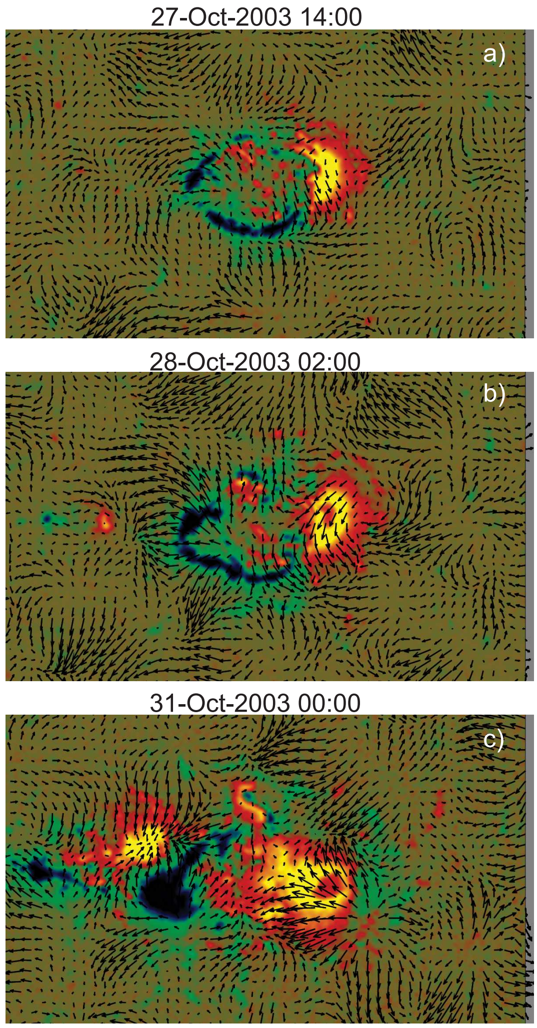

Fig. 4 Evolution of subsurface flows at the depth of 2 Mm below the photosphere during the emergence and growth of AR 10488, on 27–31 October, 2003. The flow maps are obtained by the time-distance technique using 8-hour time series of full-disk Doppler images from SOHO/MDI. The maximum horizontal velocity is approximately 1 km/s. The background image is the corresponding photospheric magnetogram (red and blue areas show regions of positive and negative polarity of the line-of-sight magnetic field.

background color maps show the corresponding magnetograms.

During the initial emergence a ring-like magnetic field structure is formed (Fig. 4). Within this structure the flows are clearly suppressed, and they remain suppressed during further evolution. Also, at the same type a diverging flow pattern starts developing at the boundaries of the magnetic structures. This pattern is consistent with the expectation that the emerging magnetic structure pulls plasma outside. Similar diverging flows associated with emerging magnetic regions have been observed on the solar surface [18, 19]. The divergent flow field becomes stronger as the active region grows (Fig. 4*b*), but later, it is replaced by a converging flow pattern around the sunspots (Fig. 4*c*). This was previously observed beneath sunspots [3].

The strength of the divergent flows is obviously

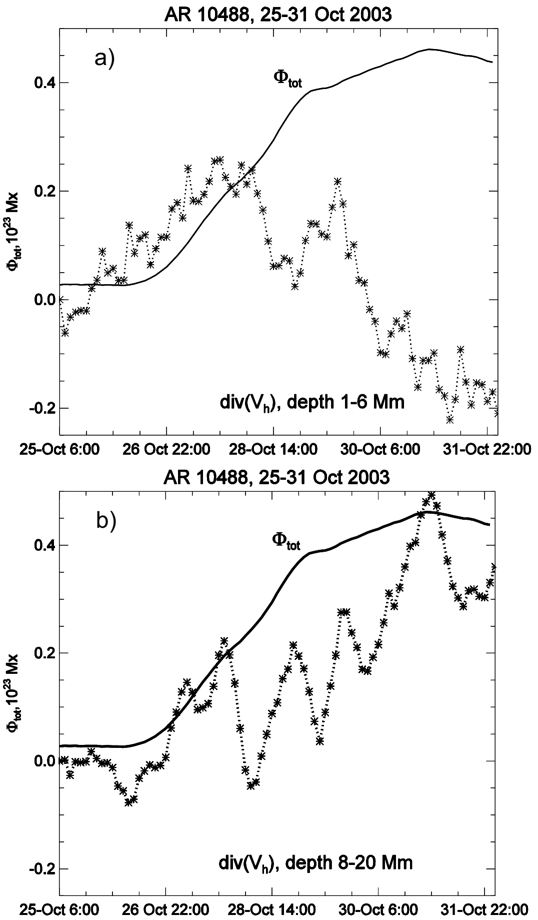

Fig. 5 The evolution of the total unsigned photospheric magnetic flux (solid curve) and the mean divergence of the horizontal flow velocity (dotted curve with stars) at the depth of 1–6 Mm (*a*) and 8–20 Mm (*b*) in the region of flux emergence of AR 10488.

related to the development of active regions, and may provide us with a prediction of their future evolution. The time evolution of the mean horizontal divergence in the two depth intervals and the photospheric magnetic flux is shown in Figure 5. It is quite clear that the horizontal velocity divergence at the depth 1–6 Mm starts to grow before the magnetic flux and reaches maximum in the middle of the flux growth phase. Then, the divergence becomes negative meaning that the flow pattern is dominated by converging flows. At greater depths, 8–20 Mm (Fig. 5*b*), the horizontal flow behavior is not very clear, probably because of higher noise, or because the flow pattern is not as well organized as in the shallower subsurface (6 Mm deep) layer. Perhaps the most significant feature at this depth is the formation of a divergent flow pattern approximately at the time of the formation of convergent flows in the upper subphotospheric layer.

One would expect that during the emergence the plasma is not only pushed outside the magnetic field area but also upward, particularly, in the upper layers.

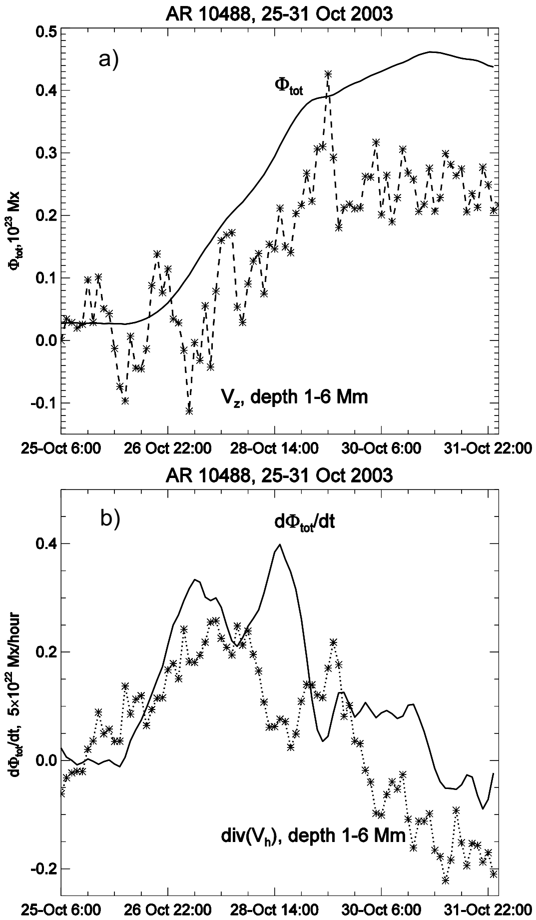

Fig. 6 *a*) The evolution of the total unsigned photospheric magnetic flux (solid curve) and the mean vertical velocity in km/s (dotted curve with stars) at the depth of 1–6 Mm in the region of the flux emergence of AR 10488. The negative velocity corresponds to upflows, and the positive velocity corresponds to downflows. *b*) The corresponding changes of the total emerging flux rate and the mean divergence of the horizontal flow components.

Observations of the line-of-sight Doppler velocity of the surface plasma have revealed relatively small-scale transient upflows in emerging active regions [19, 20, 21, 22]. Figure 6*a* shows the evolution of the mean vertical flow below the active region at the depth 1–6 Mm. Indeed, upflows dominate at the very beginning of the magnetic flux emergence. However, the signal fluctuates, reflecting a complicated structure of the vertical flows. After the emergence phase the vertical flow pattern is dominated by downflows, which are organized around the sunspots.

It seems that the horizontal divergence of subsurface flows is the most sensitive characteristic of the emerging magnetic flux. The divergent flows appear before the initial flux emergence, and continue to evolve in correlation with the magnetic flux.

Figure 6*b* shows a comparison of the mean divergence of the horizontal flows and the total magnetic flux emergence rate. Evidently, there were two or three peaks of the magnetic emergence rate. The flow divergence shows two peaks, which are anticorrelated to the flux rate. The decrease of the flow divergence during the periods of the highest magnetic flux emergence rate suggests that the emergence of new magnetic flux tubes in the sunspot region result in enhancement of converging flows, and thus, enhance the stability of the sunspot. However, the physical mechanism for this relationship is unclear.

4. Discussion

The plasma dynamics in magnetic sunspot regions of the Sun is very complicated. The helioseismology results for a large developing active region reveal large-scale outflows beneath the surface during most of the emergence phase, and also formation of converging flows around the magnetic structure of sunspots. However, the structure of the vertical flows remains unclear. There is an indication of upflows mixed with downflows at the beginning of emergence, but then the downflows dominate. In the case of AR 10488, there were two or three major flux emergence events. The photospheric magnetic flux rate and subsurface flow divergence show two or three peaks, which are in antiphase. Thus, increases of the magnetic flux emergence rate may reduce the flow divergence and prevent the magnetic flux from spreading. The observations seem to suggest that the multiple flux emergence events play important role in the formations and maintaining the magnetic structure of the large active region and sunspots. For understanding these observational results it is important to develop radiative MHD models for the dynamics of magnetic structures in the turbulent plasma.

[1] A. B. Severny, Soviet Astronomy **9**, 171 (1965).
[2] E. N. Parker, Astrophys. J. **230**, (1979).
[3] J. Zhao, A. G. Kosovichev and T. L. Duvall, Jr., Astrophys. J., **557**, 384 (2001).
[4] N. E. Hurlburt and A. M.Rucklidge, Monthly Notices of the Royal Astronomical Society **314**, 793 (2000).
[5] M. Rempel, M. Schuessler and M. Knoelker, 2008. *Radiative MHD simulation of sunspot structure.* ArXiv e-prints **808**, arXiv:0808.3294.
[6] T. L. Duvall, Jr., S. M. Jefferies, J. W. Harvey and M. A. Pomerantz, Nature, **362**, 430 (1993).
[7] T. L. Duvall, Jr., et al., Nature, **379**, 235 (1996).
[8] A. G. Kosovichev, Astrophys. J., **461**, L55 (1996).
[9] A. G. Kosovichev and T. L. Duvall, Jr., in Pijpers, F.P., Christensen-Dalsgaard, J. & Rosenthal, C.S., eds, *SCORe'96 : Solar Convection and Oscillations and their Relationship* (Kluwer) p. 241 (1997).
[10] A. C. Birch and A. G. Kosovichev, Solar Phys. **192**, 193 (2000).
[11] A. G. Kosovichev and T. L. Duvall, Jr. in *Society of Photo-Optical Instrumentation Engineers (SPIE) Conference Series* **4853**, 327 (2003).
[12] D. O. Gough, in Zahn, J.-P. & and Zinn-Justin, J., eds, *Astrophysical Fluid Dynamics* (Elsevier Science Publ.), p. 339, (1993).
[13] P. H. Scherrer, et al. Solar Phys., **162**, 129 (1995).
[14] A. G. Kosovichev and T. L. Duvall, Jr. In: R. Howe, R. W. Komm, K. S. Balasubramaniam, and G. J. D. Petrie (eds.): *Subsurface and Atmospheric Influences on Solar Activity*, *Astronomical Society of the Pacific Conference Series* **383**, 59 (2008).
[15] A. G. Kosovichev, T. L. Duvall, Jr., and P. H. Scherrer, Solar Phys., **192**, 159 (2000).
[16] J. M. Jensen, T. L. Duvall, Jr., B. H. Jacobsen and J. Christensen-Dalsgaard, Astrophysical J. **553**, L193 (2001).
[17] S. Couvidat, A. C. Birch and A. G. Kosovichev, Astrophysical J. **640**, 516 (2006).
[18] L. H. Strous, G. Scharmer, T. D. Tarbell, A. M. Title and C. Zwaan, Astron. Astroph. **306**, 947 (1996)
[19] H. Kozu, R. Kitai, D. H. Brooks, H. Kurokawa, K. Yoshimura and T. E. Berger, Publ. Astron. Soc. Japan **58**, 407 (2006).
[20] A. Pevtsov and J. B. Lamb, in *Solar MHD Theory and Observations: A High Spatial Resolution Perspective* **354**, 249 (2006).
[21] V. M. Grigor'ev, L. V. Ermakova and A. I. Khlystova, Astronomy Letters **33**, 766 (2007).
[22] A. G. Kosovichev, to be published in Space Science Reviews (2009).